1　　　　　　**Changes in water age and source during dry-down of a non-perennial stream**

2

3　**Co-author list**: Logan J. Swenson[1,2,*], Sam Zipper[1,*], Delaney M. Peterson[3], C. Nathan Jones[3], Amy J.

4　Burgin[4], Erin Seybold[1], Matthew F. Kirk[5], Camden Hatley[1,2]

5

6　**Affiliations:**

7　　　　1.　Kansas Geological Survey, University of Kansas

8　　　　2.　Department of Geology, University of Kansas

9　　　　3.　Department of Biological Sciences, University of Alabama

10　　　　4.　Kansas Biological Survey-Center for Ecological Research, University of Kansas

11　　　　5.　Department of Geology, Kansas State University

12　* Corresponding authors: loganswenson@ku.edu, samzipper@ku.edu

13

14　**Author ORCiD IDs:**

15　Swenson: 0000-0003-4981-3478

16　Zipper: 0000-0002-8735-5757

17　Peterson: 0000-0002-3444-4772

18　Jones: 0000-0002-5804-0510

19　Burgin: 0000-0001-8489-4002

20　Seybold: 0000-0002-0365-2333

21　Kirk: 000-0001-5562-7618

22　Hatley: 0000-0001-9840-2734

23

24　***This is a non-peer-reviewed manuscript being submitted to Water Resources Research.***

25

26　**Key points**:

27　　　● Stream isotopic composition was progressively enriched in $\delta^{18}O$ and δ^2H as the stream network

28　　　　dried.

29　　　● Stream isotopic enrichment is caused by evaporative effects and a decrease in surface water

30　　　　connectivity.

31　　　● Most streamflow was young water (stored in the subsurface < 3 months), with older and more

32　　　　variable water age as the stream network dried.

Abstract:

Non-perennial streams, which lack year-round flow, constitute more than half the global stream network length. Identifying the sources of water that sustain flow in non-perennial streams is necessary to understand their potential impacts on downstream water resources and inform current policy and management. Here, we used water isotopes ($\delta^{18}O$ and $\delta^{2}H$) to partition the evolution of streamwater age compositions and inferred sources through the 2021 summer dry-down period of a non-perennial stream network at the Konza Prairie (KS). During dry-down, the isotopic composition of non-perennial streams was progressively enriched in $\delta^{18}O$ and $\delta^{2}H$. Integrating two different isotope-based models of water age, we found a substantial amount of summer streamflow (median 54.4%) is young water that had been stored in the subsurface for less than 3 months. Streamwater shifted to older sources and variability in age increased as summer progressed. The shift in water age suggests a shift away from rapid fracture flow towards slower matrix flow that creates a sustained but localized surface water presence during the driest parts of the summer. Further, our analysis suggests that unmixing-based approaches are well-suited for estimating water age in non-perennial systems that lack year-round flow necessary for fitting time series-based models. The substantial proportion of young water highlights the vulnerability of non-perennial streams to short-term hydroclimatic change, while the late-summer shift to older water reveals a sensitivity to longer-term changes in groundwater dynamics. Combined, this suggests that local changes may propagate through non-perennial stream networks to influence downstream water availability and quality.

52   **Plain Language Summary**:

53   Non-perennial streams, which periodically cease to flow, are widespread globally. Identifying where the

54   water in non-perennial streams comes from and how long it takes to get to the stream is important for

55   developing water policy and management strategies. We used water isotopes ($\delta^{18}O$ and $\delta^{2}H$), a common

56   hydrologic tracer, to identify stream water sources and age during the 2021 summer dry-down period of

57   a non-perennial stream network at the Konza Prairie (Kansas, USA). We found that water sources and

58   flowpaths changed as the stream network dried. Approximately half of summer streamflow is young

59   water, meaning it took less than 3 months to travel from precipitation to the stream. However, as the

60   summer progressed, streamwater shifted to older sources. We interpret this shift in the water age to

61   indicate a shift in the source of water from rapid flowpaths early in the summer, to slower flowpaths

62   later in the summer, which sustain localized surface water during the driest parts of the year. Taken

63   together the substantial amount of young water highlights the vulnerability of non-perennial streams to

64   short-term weather changes and longer-term changes in groundwater dynamics that may propagate

65   through non-perennial stream networks to influence downstream water availability and quality.

1. Introduction

Non-perennial streams, including intermittent and ephemeral streams, which do not flow year-round (Busch et al., 2020), constitute more than half the global stream network length (Messager et al., 2021), and are becoming more common worldwide (Zipper et al., 2021; Tramblay et al., 2021). Non-perennial streams are important because they influence the ecological health of river networks through regulation of biogeochemical cycles of nutrients and organic matter (Hale and Godsey, 2019; Zimmer and McGlynn, 2018) and local and downstream water quality and quantity (Gómez et al., 2017). Despite their prevalence and importance, non-perennial streams are overlooked and understudied (Krabbenhoft et al.,2022); however, growing recognition of their abundance has driven attempts to refine hydrological and ecological theories to account for the unique characteristics of non-perennial flow regimes (Shanafield et al., 2021; Allen et al., 2020).

While a growing number of recent studies have highlighted the important and unique role of non-perennial streams in watershed hydrologic and ecological function, management of and policy affecting these systems remains contested and unclear (Walsh and Ward, 2022). Part of the ongoing policy debate regards defining which non-perennial water bodies have a significant connection to downstream perennial streams (Ward et al. 2023). Repeated disagreement over how to define "significant connections" persists (Alexander, 2015), as seen in policy that extends protections to adjacent waters on a case-by-case basis if they have a "significant nexus" (Clean Water Rule, 2015) or if they contribute continuous flow to downstream perennial waters (Navigable Waters Protection Rule, 2020). Both of these rules have since been repealed or vacated, with US federal protections returning to those codified by the US EPA and ACE in 1986 (US DOD, 1986; Wade et al. 2022). These policy changes and debate suggest an urgent need to quantify the influence of non-perennial streams on both local and downstream water quantity and quality (Koundouri et al., 2017; Stubbington et al., 2020).

Quantifying the connection between non-perennial streamflow and water quality first requires an understanding of the origin of water in these streams and the timescales over which water is transmitted to the stream (Hrachowitz et al., 2016). Addressing this knowledge gap is challenging because most of our understanding of water sources comes from perennial streams where ages are integrated at the catchment outlet over larger temporal scales, commonly annual timesteps (Segura, 2021; Lutz et al., 2018; Jasechko et al., 2016). However, aggregating age estimates at an annual resolution does not reflect the finer-scale temporal variability of water sources in non-perennial streams, which often flow seasonally or in response to precipitation events (Shanafield et al., 2021; Costigan et al., 2016). Furthermore, many previous water age and source estimates often integrate age

98   and source to a single measurement point at the watershed outlet, thereby failing to capture the

99   potential variation in the spatial distribution of water within a network (Jensen et al., 2019; Botter and

100   Durighetto, 2020). Thus, quantifying the within-network spatial and temporal evolution of water age

101   and sources in non-perennial streams underpins our ability to predict the vulnerability of these systems

102   to changes in groundwater dynamics and streamflow which are exacerbated by changing climate and

103   human activities (Zipper et al., 2022; Datry et al., 2022). Ultimately, understanding where and when

104   there is water in non-perennial streams, and the source of that water, addresses the extent to which

105   they are connected to downstream waters.

106   To address this knowledge gap, our goal was to quantify the spatiotemporal variability in stream

107   isotopic composition and water age, and infer changes in water source during the dry-down of the

108   stream network for a non-perennial stream at the Konza Prairie Biological Station (Kansas, USA).

109   Specifically, we asked three questions: (1) How do streamwater isotopic compositions in non-perennial

110   streams vary spatially and temporally? (2) What factors most strongly influence the distribution of

111   isotopic compositions in non-perennial streams, and how do these factors vary through time? (3) What

112   does this imply about the sources of water and their transit times sustaining streamflow? We answered

113   these questions using water isotopes (δ^{18}O and δ^{2}H), a commonly applied hydrologic tracer for

114   identifying water sources and modeling water age (Jasechko, 2019), that were collected through regular

115   sampling at the watershed outlet and three spatially-dense synoptic campaigns throughout summer

116   2021. The water isotope data were used in models of water mixing and young water fraction to partition

117   the sources of water sustaining streamflow in a non-perennial stream and to estimate timescales of

118   storage within the watershed.

119

120   **2. Data and Methods**

121   **2.1. Study Site**

122   This study analyzes the 2021 summer dry-down of Kings Creek at the Konza Prairie Biological

123   Station in the Flint Hills of Kansas, USA (Figure 1). Konza Prairie is a native tallgrass prairie, part of the

124   National Ecological Observatory Network (NEON) and is a Long Term Ecological Research (LTER) site. The

125   terrain is merokarst with thin limestone units (1-2 m thick) interbedded with mudstone/shale units (2-4

126   m thick), and is characterized by flashy stream responses to precipitation events, preferential flow

127   through conduits, and strong vertical heterogeneity (Sullivan et al., 2020; Vero et al., 2018; Macpherson

128   1996). The landscape is terraced with more resistant limestone units forming benches on hillslopes and

129   knickpoints in stream channels, while less resistant mudstones erode to more gradual slopes (Costigan

130   et al., 2015). Soils are predominantly silty-clay loams; however, bedrock commonly outcrops at the

131   surface (US soil taxonomic system; Ransom et al., 1998). Soil profiles are deepest at the base of slopes

132   (~2 m) and are thinnest on the ridges (<20-50 cm) (Ransom et al., 1998).
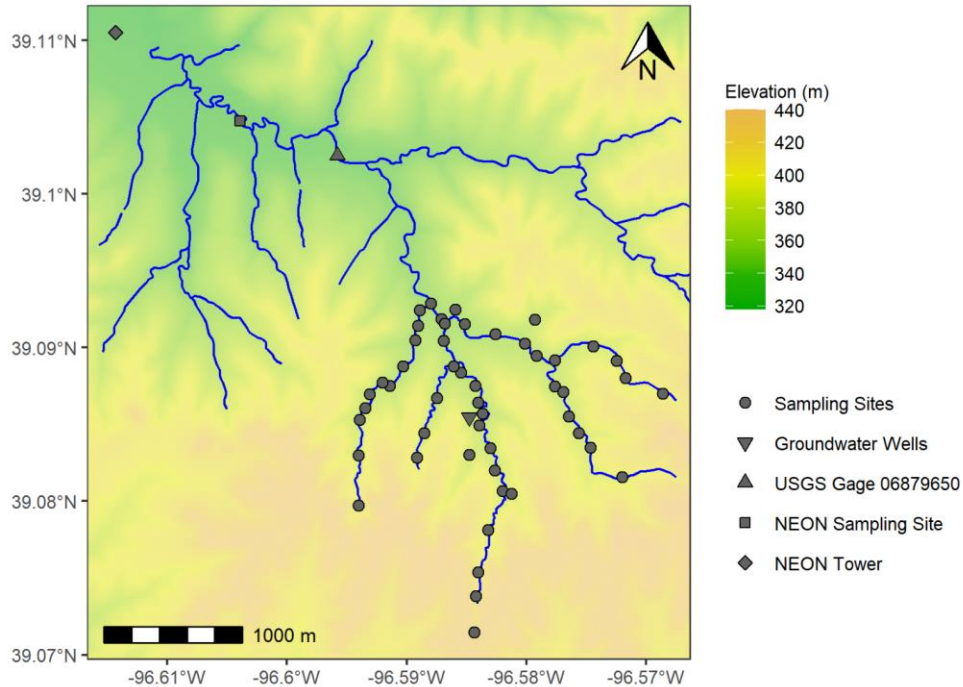
133

134   **Figure 1**. Stream sampling sites and infrastructure along Kings Creek in the Konza Prairie, KS, USA. Note:

135   The groundwater wells are offset 50 m away from the stream to be visible.

136

137   The climate is mid-continental with cold, dry winters and warm, humid summers (Vero et al.,

138   2018). Average annual precipitation is 835 mm, with ~75% of rainfall occurring between April and

139   September, when vegetation is active and evapotranspiration rates are high (Hayden, 1998). Konza

140   Prairie received 632 mm in the 2021 calendar year (76% of the annual average, Figure 2). 1150 ha of tall

141   grass prairie is drained by Kings Creek, a fifth order stream which has been monitored by the USGS since

142   1979 (USGS gage 06879650). The Kings Creek network dries in many, but not all, years between

143   approximately July and September due to a decrease in precipitation and increase in evapotranspiration

144   (Costigan et al., 2015). Groundwater wells are screened in the Upper and Lower Eiss and Morrill

145   limestone units which contribute considerable amounts of groundwater to the stream at mid-elevations

146   in the South Fork of Kings Creek via springs along the hillslopes and within the streambed (Hatley et al.,

147   2022). Due to the karstic nature of these limestone units and potentially well-developed stream-aquifer

148   connections, discharge and groundwater levels respond quickly to precipitation events (Hatley et al.,

149   2022; Brookfield et al., 2016). Based on pressure responses in the groundwater wells, the Upper Eiss

150   Limestone appears to have slightly higher conductivity than the Morrill Limestone, with both having

151   greater conductivity and stream connectivity than the Lower Eiss Limestone (Figure 2; Hatley et al.,

152   2022).
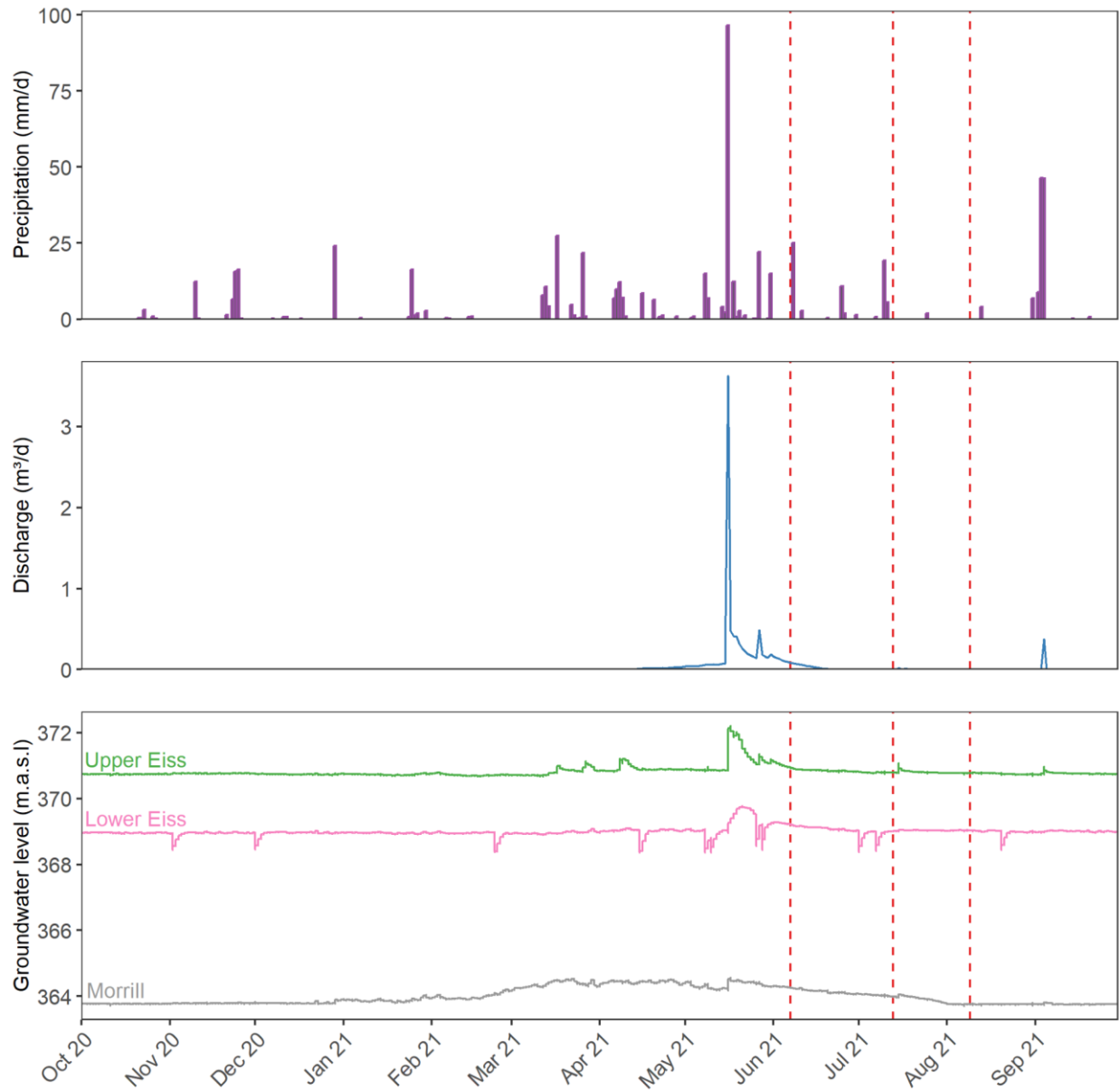
153

154   **Figure 2**. Timeseries of (a) precipitation, (b) discharge at USGS gage 06879650, and (c) groundwater

155   levels at the Konza Prairie. Sampling events are shown as vertical dashed lines. Sharp declines in

156   groundwater levels in the Lower Eiss occurred as a result of periodic sampling events.

157

2.2. Sampling Design & Ancillary Data

Water isotopes ($\delta^{18}O$ and $\delta^{2}H$) were collected on June 7th, July 13th, and August 9th (2021) as part of three synoptic campaigns designed to capture a range of surface water connectivity conditions during the dry-down of a non-perennial stream network. We identified 50 sampling sites spanning a range of drainage area and topographic wetness index, which have been previously shown to be significant predictors of flow permanence in non-perennial streams (Warix et al., 2021). A subset of the locations strategically targeted sites with long-term data, known springs, and other locations of interest (see supplemental section SI1.1 for full details on the sampling design). The synoptic samples were collected only on the South Fork of Kings Creek; the most downstream synoptic network sampling point, representing a drainage of 531 ha. On each sampling date, we visited all 50 sampling sites and collected samples if water was present, along with ancillary information regarding the hydrologic conditions (i.e., whether the water was flowing or pooled and water temperature). A total of 77 distinct grab samples, excluding duplicates, were obtained: 43 samples in June, 19 samples in July, and 15 samples in August. All samples were stored in 60-mL glass vials with conical inserts and capped without headspace in order to prevent isotopic fractionation. Samples were kept in dark and at room temperature (<20 °C) until analysis.

Additional data were leveraged from the US Geological Survey (USGS), National Ecological Observatory Network (NEON), and the Konza Prairie Long Term Ecological Research (LTER) programs. Discharge in Kings Creek was obtained from USGS gage 06879650, which is ~1.6 km downstream from the most downstream point of our synoptic sampling. Composite precipitation isotopes were collected approximately every two weeks between November 2018 and September 2021 from a wet deposition collector at the NEON Tower, with a gap in collection from March 2020 to July 2020 during the onset of the COVID-19 pandemic (n = 45; Figure 1; NEON, 2022). The precipitation-sampling collectors meet International Atomic Energy Agency (IAEA) recommendations to prevent evaporation. In addition to the precipitation isotopes, stream isotopes were collected approximately every two weeks over the 2021 water year at the NEON Sampling Site (n = 22; Figure 1; NEON, 2022), which is ~1.1 km downstream of the USGS gage, and has a contributing area of 1306 ha. The USGS and NEON measurement points had substantially larger contributing areas, incorporating both the North and South Fork of Kings Creek, while the synoptic samples were only in the South Fork. NEON precipitation and stream isotopes were stored in dark, cool (<20 °C) conditions and analyzed at the SIRFER Lab at University of Utah. Daily precipitation amounts were recorded at the Konza Prairie Headquarters meteorological station (Figure 1; Nippert, 2022). Groundwater levels were logged at 5-min intervals in the Upper Eiss, Lower Eiss, and

190   Morill limestone aquifers (Figure 1; Hatley et al., 2022). The meteorological and groundwater data

191   collection networks are maintained by the Konza Prairie LTER program.

192

193   **2.3. Lab Analysis**

194   Surface water isotopes were measured using a cavity ring-down spectroscopic isotopic water

195   analyzer (Picarro L2130-*i,* Picarro Inc., CA). All samples were calibrated against internal secondary

196   standards, and secondary standards were calibrated against the IAEA primary standards for Vienna

197   Standard Mean Ocean Water (VSMOW; $\delta^{18}O$ = 0.0‰, δ^2H = 0.0‰). Average instrument precision was

198   calculated as 0.05‰ and 0.41‰ for $\delta^{18}O$ and δ^2H respectively based on the comparison of 41 total

199   duplicate internal standard samples. Isotopes values were reported in parts per thousand (‰) deviation

200   relative to VSMOW:

201                                    $$\delta = ((R_s/R_{std}) - 1) * 1000$$

202   where R_s and R_{std} are the isotope ratio ($^2H/^1H$ or $^{18}O/^{16}O$) in the samples and standard (VSMOW)

203   respectively (Craig, 1961).

204   Deuterium excess (d-excess) was calculated for each sample as *d-excess* = δ^2H - 8 x $\delta^{18}O$, where

205   d-excess values less than 10 (i.e., the intercept of the Global Meteoric Water Line) indicate a sample has

206   been partially evaporated (Dansgaard, 1964).

207

208   **2.4. Data Analysis**

209   In this study, we integrated two different approaches to estimate water age, leveraging both

210   spatial and temporal characteristics of our dataset. For the synoptic samples, we conducted a point-

211   based water age estimation using a Bayesian unmixing approach that takes advantage of our spatially-

212   dense, but temporally limited data (Section 2.4.1). Using long-term NEON data, we used seasonal

213   amplitude ratios of precipitation and streamflow isotopes to estimate the fraction of young water at the

214   catchment outlet integrated across the 2021 calendar year (Section 2.4.2). For comparison between the

215   two methods, we also applied the Bayesian unmixing approach to the long-term NEON samples

216   collected at the catchment outlet. Combining these two approaches allows us to investigate both the

217   spatial dynamics and average catchment outlet processes of water age, as well as the extent to which

218   these two approaches are comparable in non-perennial streams.

219

2.4.1. Approach 1: Bayesian Unmixing

We used the mixing-evaporation model of Bowen *et al.* (2018) to infer the relative age of streamwater at each sampling point during drying. In doing so, we assumed that the isotopic signal in streamwater reflects an integrated mix of seasonally-distinct precipitation signals, dependent on their pathways to streamflow. We defined two amount-weighted sources contributing to streamflow: (1) precipitation that fell less than ~3 months ago and (2) precipitation older than 3 months. These age bins were selected to match the catchment-integrated young water fraction approach described in Section 2.4.2.

The mixing-evaporation model (*mixSource*) is available in the *isoWater* package in R (Bowen, 2022) and uses Markov Chain Monte Carlo sampling to generate a posterior distribution of source mixtures conditioned on the observed isotopic values. Prior distributions for the isotopic signal in precipitation and the local evaporation line were provided to the package. The slope of the evaporation line (m = 6.00 ± 0.55) was estimated as a linear regression fit to the stream isotopes during the summer dry-down (Figure S5). The prior describing the relative contributions of each source was left uniformed. For all analyses, three chains were generated, each run to a length of 200,000 samples with thinning to retain 7,500 samples per chain. Convergence was assessed with the R-hat statistic (R-hat < 1.05) and effective sample size (mean = 930), indicating good model convergence.

2.4.2. Approach 2: Young Water Fraction (F_{YW})

Streamwater's isotopic signal is typically damped and lagged relative to the seasonal cycle of precipitation isotopes, reflecting catchment storage and transit times (Kirchner, 2016a). The seasonal isotopic signal in precipitation (A_P) and streamwater (A_Q) can be described as:

$$\delta^{18}O_P(t) = \underline{\delta^{18}O_P} + a_P cos(ct) + b_P sin(ct) \qquad \text{\{Eq. 1\}}$$

$$\delta^{18}O_Q(t) = \underline{\delta^{18}O_Q} + a_Q cos(ct) + b_Q sin(ct) \qquad \text{\{Eq. 2\}}$$

where $\delta^{18}O_P(t)$ and $\delta^{18}O_Q(t)$ are the isotopic values in precipitation and streamwater at time t, $\underline{\delta^{18}O_P}$ and $\underline{\delta^{18}O_Q}$ are the mean isotopic values in precipitation and streamwater, and c is the radial frequency constant (0.017214 rad/day). Both $\delta^{18}O_P(t)$ and $\delta^{18}O_Q(t)$ values were amount weighted to give less weight to periods of low-precipitation and to periods of zero-discharge when isotopes were collected from isolated pools. Following von Freyberg *et al*. (2018), the coefficients a and b were obtained using iteratively reweighted least squares regression, a robust estimation method that gives less weight to

250   outliers. From this, the young water fraction (F_{YW}) was calculated as the amplitude ratios of $\delta^{18}O$ in

251   streamwater and precipitation:

252 $$F_{YW} = A_Q/A_P \ = \frac{\sqrt{a_Q{}^2 + b_Q{}^2}}{\sqrt{a_P{}^2 + b_P{}^2}} \qquad \{Eq. 3\}$$

253   The F_{YW} is a metric proposed by Kirchner (2016a) that quantifies the percentage of streamflow less than

254   approximately 2.3 ± 0.8 months in age for a wide range of catchment transit time distributions.

255   Compared to other measures of water age, such as mean transit times, the F_{YW} is not prone to

256   aggregation error bias and can be quantified even in catchments that are heterogeneous and

257   nonstationary (Kirchner, 2016a; Kirchner, 2016b). However, because it relies on fitting sinusoidal models

258   to stream isotope values (Eq. 2), it is unclear how well it would perform in a non-perennial stream where

259   water samples are not available year-round. Uncertainty in F_{YW} was assessed by generating random

260   errors in the original precipitation and streamwater isotope data (Lutz et al., 2016). The original data

261   were disturbed using a normal distribution of the random errors with a standard deviation equal to 5%

262   of the range of observed $\delta^{18}O$ values. The F_{YW} was calculated 10,000 times (Eq. 3) by fitting the disturbed

263   data to sinusoidal models for $\delta^{18}O_P(t)$ and $\delta^{18}O_Q(t)$ (Eq. 1 and 2), respectively.

264

265   **3. Results & Discussion**

266   **3.1. Spatiotemporal Patterns in Stream $\delta^{18}O$ Compositions**
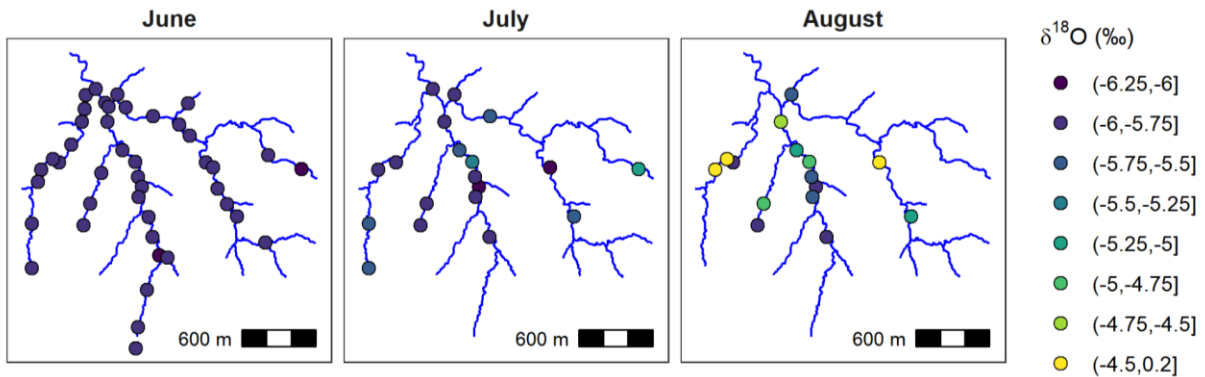
267

268   **Figure 3**. Spatial variation in $\delta^{18}O$ during the summer dry-down period.

269
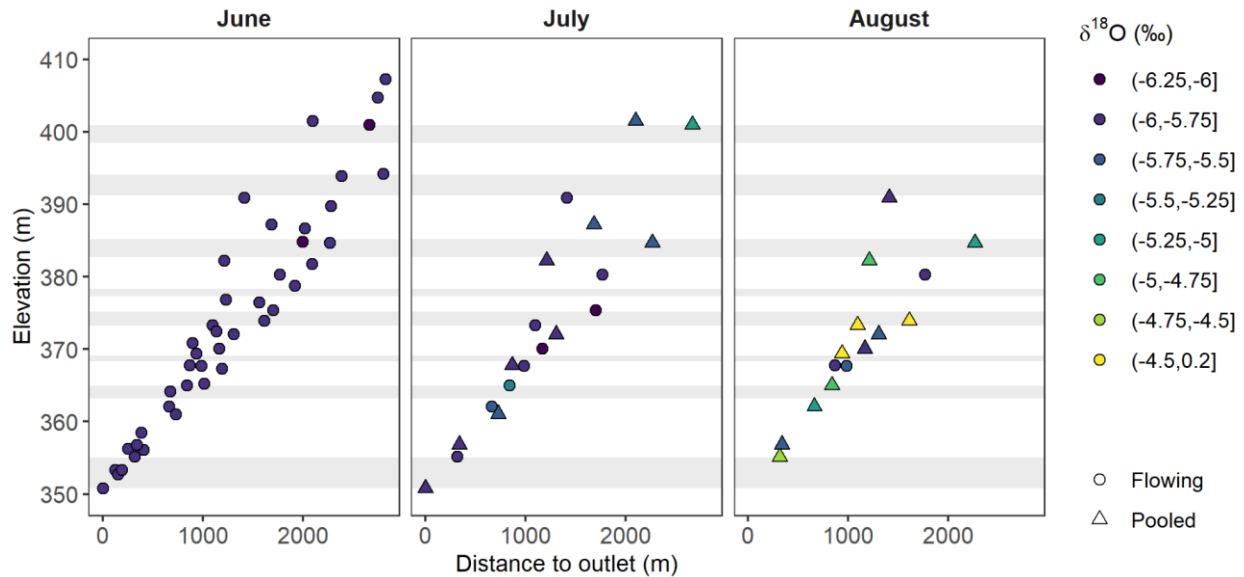
Figure 4. Variation in δ¹⁸O with distance to outlet during the summer dry-down period. Elevations where limestone units outcrop the watershed are shown as gray bands. These elevations are based on average member thickness in the drilling log records at the Konza Prairie.

Over June, July and August 2021, the South Fork of Kings Creek shifted from a fully flowing, connected system to a network of isolated pools concentrated in mid-elevations (Figure 3, Figure 4). The stream network went from 86% wet in June, to 38% wet in July, to 30% wet in August (Figure 3). Stream drying occurred between June and August at elevations below ~355m and above ~390m, while mid-elevations in the watershed remained wet (Figure 4). Stream drying fragmented the network into a series of flowing reaches and isolated pools, with pools representing most of the surface water in August (Figure 4). Based on past studies that have linked flow to storage thresholds in the underlying limestone aquifers (Costigan et al., 2015; Hatley et al., 2022), we interpret this widespread wet to dry transition as a reversal of stream-aquifer direction during the summer. Localized points of drying are likely where the stream transitioned from gaining to losing at that location and/or upstream, while points where flow is sustained throughout the summer are likely at or immediately downstream of persistent groundwater discharge points.

Surface water persisted at elevations in the range of several limestone aquifers, including the Eiss and Morill aquifers (Figure 4). The thin 1 - 2 m karstified limestone formations are thought to be the primary source of water sustaining flow in the South Fork of Kings Creek (Hatley et al., 2022; Keen et al., 2022; Sullivan et al., 2019). Hatley et al. (2022) found groundwater discharge contributed up to 96.3% of streamflow during their sampling events, which spanned from April through July (2021), with minimal

291 streamflow sourced from soil water (0.13%) and surface runoff (3.83%). Konza's alternating karstified

292 limestone formations sustain surface water presence where they outcrop at mid-elevations in the

293 watershed during the driest parts of the year. Groundwater is known to sustain flow in a range of

294 systems from small headwater non-perennial streams (Hatley et al., 2022; Warix et al., 2021) to large

295 intermittent rivers (Zipper et al., 2022; Vu et al., 2018). In instances where regional hydrological regime

296 drivers are unimportant, such as in the South Fork of Kings Creek, it is local groundwater and its

297 bidirectional flow to the stream that controls flow permanence and produces nuanced wetting and

298 drying patterns in space and time (Zimmer and McGlynn, 2017).

299 The δ^{18}O composition of streamwater was progressively enriched during the network dry-down

300 and variability in δ^{18}O increased considerably over the summer months (Figure 3). Stream δ^{18}O ratios in

301 the headwaters varied in space and time, ranging from -6.01‰ to -5.75‰ in June, -6.13‰ to -5.10‰ in

302 July, and -5.92‰ to 0.18‰ in August (Figure 3). We infer the stream to be well connected and gaining

303 groundwater from the limestone aquifers in June, when stream δ^{18}O compositions are similar across the

304 network and the stream was flowing at all sampling points. However, as the limestone aquifers drained

305 out in the dry summer weather and stream-aquifer directions reversed, disparate portions of the

306 watershed in space and time were disconnected from groundwater inputs, and the δ^{18}O signal in the

307 remaining isolated pools were enriched due to evaporative effects.

308 The within-network variability of δ^{18}O in the headwaters (-6.13‰ to 0.18‰) is wider than the

309 range of δ^{18}O observed at the downstream NEON site (-6.14‰ to -4.91‰) over the 2021 calendar year.

310 This comparison in variation is significant because it is often assumed that the range of stream isotopic

311 composition can be captured at an outlet with repeated sampling. However, our results indicate that

312 repeated water sampling at a catchment outlet can fail to bound the full range of δ^{18}O values. This

313 suggests that spatially dense synoptic sampling like that used here and in a limited number of other

314 studies (Ward et al., 2019; Segura et al., 2019), while effort-intensive, can provide a more nuanced

315 perspective on within-watershed dynamics and drivers of flow that are obscured by outlet-based

316 sampling approaches.

317
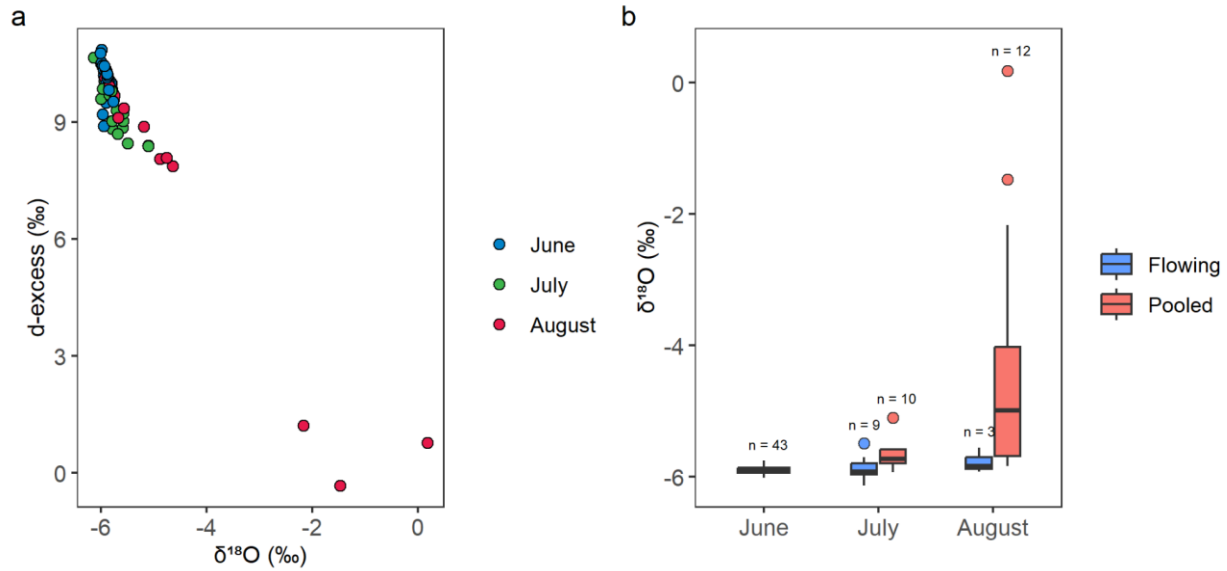
Figure 5. Variability in (a) $\delta^{18}O$ and d-excess and (b) $\delta^{18}O$ and surface water connectivity during the summer dry-down period.

There are two interrelated factors that influence the variation in water isotopic signatures: (1) evaporative effects, as indicated by deuterium excess (d-excess; Figure 5a) and (2) a decrease in surface water connectivity (Figure 5b). Deuterium excess (d-excess) ranged from 8.90‰ to 10.85‰ in June, 8.39‰ to 10.65‰ in July, and -0.32‰ to 10.12‰ in August (Figure 5a). Shifts to lower d-excess values are consistent with removal of light water vapor from the stream water during evaporation. Thus, the degree of evaporation-induced isotopic fractionation increased throughout the summer as conditions warmed and precipitation events became less frequent. These evaporative effects also produced differences in the $\delta^{18}O$ compositions of flowing reaches compared to isolated pools by the end of the summer (Figure 5b). Further, variability in $\delta^{18}O$ ratios increased as surface water connectivity decreased and stream-aquifer directions reversed towards losing water to the underlying limestone aquifers and/or awaiting evaporation in isolated pools above impermeable mudstones. In a random forest model to predict stream $\delta^{18}O$ summed over the summer months, day of year and flowing/pooled reaches were the best overall predictor for explaining observed stream $\delta^{18}O$ compositions, highlighting the role of disconnection in driving evaporation (Figure S6).

3.3. Ages and Sources of Water Sustaining Streamflow

3.3.1. Spatiotemporal variability during drydown
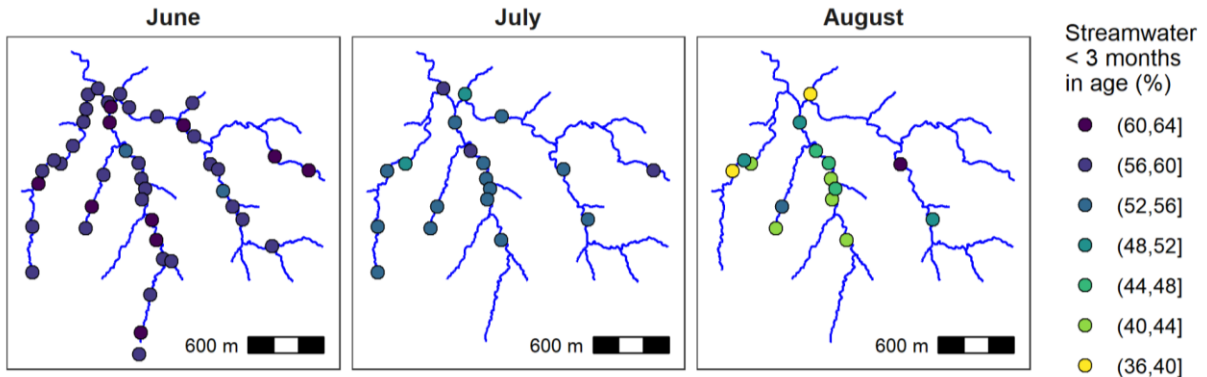
Figure 6. Percent of streamflow less than ~3 months in age estimated from Bayesian unmixing approach. Streamflow age is defined as the mean of the posterior distribution of source mixtures.

The age of streamflow generally became older and more spatially variable over the course of the summer (Figure 6). Streamflow less than ~3 months in age ranged from 53.9% to 62.6% (mean = 58.8%) during June, when the stream network was fully connected and flowing. However, as the stream became disconnected, the proportion of young streamflow decreased and ranged from 49.5% to 59.0% (mean = 54.0%) in July , and 39.1% to 62.0% (mean = 46.4%) in August (Figure 6). We interpret these results, which account for the effects of evaporation, to reflect a shift in groundwater inputs to the stream, from fast-draining flowpaths in June to more slowly draining flowpaths from lower permeability horizons later in the summer. There is minimal variation in water age in June, when most of the stream network received relatively young water from recent precipitation and flow throughout the network homogenized estimated water age.

However, as the aquifers drained out in the dry summer weather, older water sustained flows with increased variability in water age as the stream network transitioned from wet to dry and stream-aquifer directions reversed. In July and August, the percentage of older water increased, presumably from water with more varied age compositions being transported through less permeable pore space and reduced mixing due to decreased surface water connectivity (Figure 4), though network-wide approximately half of the stream water was still younger than 3 months in age. The high percentage of young water aligns with past studies that have shown preferential flow (i.e., soil macropores, fractures, solution-enlarged pores, and springs) to be important in this watershed with relatively fast flowpaths routing water to the stream (Macpherson and Sullivan, 2019; Tsypin and Macpherson, 2012;

361   Macpherson et al., 2008). Similarly high young water fractions (reaching up to 40%) and short mean

362   transit times (0.34 to 0.74 years) have been reported in other small headwater non-perennial streams in

363   karst aquifers, where young water is likely transmitted via well-developed karst conduits (Rusjan et al.,

364   2019).

365

366   **3.3.2. Implications at watershed outlet**
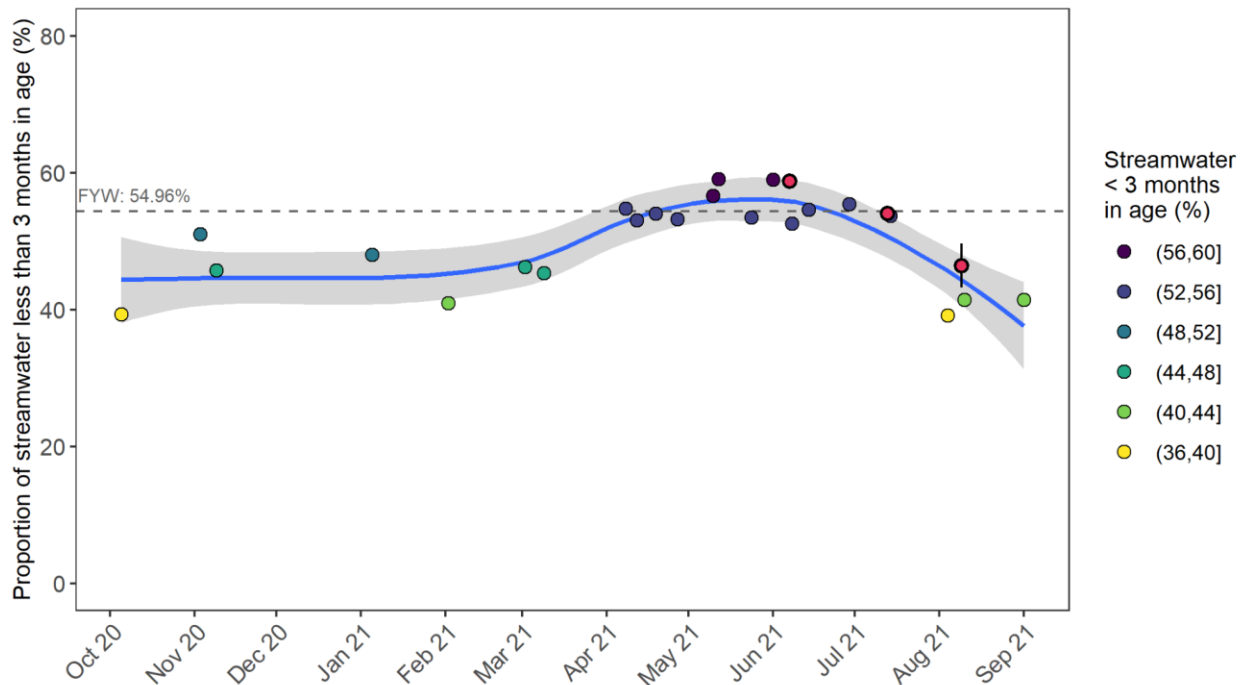
367

368   **Figure 7**. Streamflow less than ~3 months in age from Bayesian unmixing (points) and F_{YW} across the

369   2021 water year (dashed horizontal line) at the NEON sampling site. For comparison, the red dots show

370   the average and 95% confidence interval of all the synoptic sampling points (i.e., all points in Figure 3).

371   The blue line and shaded interval show a loess fit with its 95% confidence interval for the Bayesian

372   unmixing.

373

374   To evaluate the results of our unmixing approach, we compared Bayesian unmixing at the

375   downstream NEON $\delta^{18}O$ timeseries to the young water fraction (F_{YW}), which is an alternative, timeseries-

376   based method for estimating water age. The F_{YW} is a complementary metric that estimates the

377   percentage of streamflow less than 2.3 ± 0.8 months in age for a wide range of catchment transit time

378   distributions (Kirchner, 2016a). Both the Bayesian unmixing approach and F_{YW} quantify the front-end of

379   the transit time distribution for Kings Creek, meaning they measure water being transported along

380 preferential flowpaths rather than long regional flowpaths or matrix pore space. Transport along

381 regional flowpaths and through matrix pore space is often orders of magnitude slower and produces

382 typical mean transit times on the order of years or even decades (McGuire and McDonnell, 2006).

383   Water age estimates using the Bayesian unmixing approach (approach 1) applied at the

384 downstream NEON sampling site agreed well with average water age derived from fraction young water

385 (approach 2) during the summer months; both spatial and temporal water age estimates are consistent

386 with the F_{YW}. Bayesian estimates of streamflow less than ~3 months in age ranged from 39.2% to 59.1%

387 in 2021, with older water sustaining streamflows during the driest parts of the year, and agreed well

388 with the average of water age from the synoptic points (Figure 7). The median F_{YW} was 54.4% for the

389 2021 water year, with a 95% confidence interval of 38.1% to 71.4% (Figure 7; Figure S8), which is also

390 consistent with the synoptic sampling results. Thus, we observe good agreement in water age estimates

391 between the three approaches tested here: Bayesian unmixing of synoptic samples, Bayesian unmixing

392 of downstream NEON samples, and F_{YW} of NEON samples. These results suggest that the Bayesian

393 unmixing approach is a robust method for understanding water age at multiple points in a watershed

394 over timesteps smaller than the annual average provided by the F_{YW} method. Furthermore, it suggests

395 that the Bayesian unmixing method is better-suited for estimating water sources in non-perennial

396 systems, where perennially-based methods to estimate water age do not work due to lack of surface

397 water during portions of the year(e.g., fitting sinusoidal models or transit time distributions).

398

399 **3.4 Synthesizing evidence of water age and source in non-perennial streams**

400   Multiple studies have concluded that groundwater sustains flow in the South Fork of Kings Creek

401 (Hatley et al., 2022; Keen et al., 2022; Sullivan et al., 2019); however, the transit time for groundwater to

402 reach the stream remained unknown. We found the South Fork of Kings Creek shifted from a fully

403 flowing, connected system to a network of isolated pools, where surface water persisted due to

404 groundwater inputs from the many limestone aquifers (Figure 3 and 4). During the network dry-down,

405 the $\delta^{18}O$ composition of streamwater was progressively enriched due to evaporative effects and a

406 decrease in surface water connectivity (Figure 5). Multiple lines of evidence suggest that a substantial

407 amount of summer streamflow (up to 62.6% at points) originated as relatively young water sourced

408 from spring rains and high-intensity summer storms (Figure 6 and 7).

409   Streamflow in the South Fork of Kings Creek is a mixture of young and old water, with increasing

410 age as the stream network dries, indicating that old water can be stored in the subsurface but remain

411 disconnected from the stream for part of the year. Understanding this mixture of young and old water in

412   generating streamflow provides another line of evidence for the "fill and spill" hydrology hypothesized

413   to operate in the Konza Prairie and other similar merokarst settings, where storage thresholds control

414   flow permanence (Costigan et al., 2015; McDonnell et al., 2021). In brief, when the watershed is dry,

415   precipitation infiltrates into the subsurface to "fill" the many limestone aquifers, but does not push

416   groundwater to the stream. However, as the limestone aquifers exceed some critical threshold of

417   storage, they "spill" by pushing groundwater to the stream. At the point when storage thresholds are

418   exceeded, precipitation and streamflow patterns are synchronized (Costigan et al., 2015). Our results

419   suggest that spring and early summer rains provided a substantial flux of young water that was

420   transmitted to the underlying limestone aquifers through soil macropores and bedrock fractures (noted

421   in Macpherson and Sullivan, 2019; Tsypin and Macpherson, 2012; Macpherson et al., 2008) and, once

422   storage thresholds were exceeded, the stream network transitioned to flowing and connected. As the

423   stream dried, the shift in water age indicates a shift in water sources from within-year preferential

424   groundwater discharge to much older groundwater that was pushed out of less permeable matrix pore

425   space. Taken together, our study indicates that seasonal contributions of young water drive storage

426   above critical thresholds causing wet-up, while old water is more slowly pushed out of the less

427   permeable pore space thereby sustaining surface water during the driest parts of summer.

428   Groundwater plays a critical role in sustaining flows in non-perennial streams spanning the river

429   network continuum, from small headwater streams (Hatley et al., 2022; Warix et al., 2021) to large

430   mainstem rivers (Zipper et al., 2022; Vu et al., 2018). The hydrological regimes of non-perennial streams

431   are driven by a wide range of factors including meteorology, geology, land cover, and human activities,

432   which interact over a range of spatial and temporal scales to influence the quantity of groundwater

433   available to sustain flows (Hammond et al., 2020; Shanafield et al., 2021). However, by definition, non-

434   perennial streams become disconnected from groundwater inputs at some point in time throughout the

435   year. Thus, stream-aquifer interactions in non-perennial streams are bidirectional in space and time

436   (Staudinger et al., 2021), meaning that non-perennial streams can serve as focal areas of regional

437   groundwater recharge for some period of the year, while contributing water, solutes, and materials to

438   downstream perennial waters during the rest of the year. Indeed, non-perennial streams, especially in

439   karst regions, are a dynamic and critical interface between the landscape, regional aquifers, and

440   navigable waters, with far-reaching implications for water management and policy.

441

4. Conclusions

Non-perennial streams are the source of considerable debate regarding policy and management; much of the debate centers on their connection to downstream sources. Thus, our demonstration of the prevalence of relatively fast flowpaths in sustaining flow in non-perennial streams provides a structural "significant nexus" between small, non-perennial headwater streams and their downstream perennial rivers in merokarst regions. Therefore, we conclude that management decisions around non-perennial streams that alter water quality and/or quantity have the potential to "significantly affect the chemical, physical, and biological integrity" of downstream navigable waters (Clean Water Rule, 2015). Due to the predominance of fast flowpaths sustaining streamflow in Kings Creek, nutrients and contaminants have the potential to be transported over short timescales from the landscape to the stream, with little time for attenuation. These fast flowpaths could exert a disproportionate influence on downstream water quality, where young water is less prevalent. For example, in agricultural regions, nitrate from farming operations has extensively degraded surface and groundwater quality; the prevalence of fast groundwater flowpaths in regions with high legacy nitrogen load could contribute to on-going declines in surface water quality (Byrnes et al., 2020; Van Meter et al., 2018; Van Meter et al., 2016). As another example, even much longer groundwater flowpaths have been shown to rapidly transport contaminants over short timescales (< 10 months), as seen in the contentious County of Maui, Hawaii v. Hawaii Wildlife Fund case (Cornwall, 2020; Craig et al., 2013). Degradation of water quality could be further compounded by changes in water availability driven by short-term hydroclimatic change and longer-term changes in groundwater dynamics, which could cause downstream perennial waters to receive increasingly variable streamflows, with potential to affect our ability to meet both agricultural and domestic water requirements. Indeed, policymakers and water managers may need to account for the potential fast transit of water from the landscape to non-perennial streams to downstream perennial waters, which suggests that upstream alterations of land use and climate have the potential to shift downstream water quality and quantity.

We combined water isotopes with isotope-based models of water mixing and young water fraction to partition water age, water source, and associated changes during the summer dry-down of a non-perennial headwater stream network at the Konza Prairie. We found pronounced spatial and temporal variability in stream $\delta^{18}O$ compositions during the summer dry-down period due to evaporative effects and a decrease in surface water connectivity. Water age estimates from two independent datasets are similar, and in agreement with the F_{YW} age estimates, suggesting that our Bayesian Unmixing approach is a robust method for understanding water age at multiple points in a

watershed over timesteps smaller than a year. We found that a substantial amount of streamflow in the South Fork of Kings Creek originated as young water sourced from within-season precipitation that had been stored in the subsurface for less than 3 months, regardless of position in the watershed. As the summer progressed, there was a shift to older water sources, with variability in age compositions distributed throughout the drying stream network. We interpret this water age transition as a shift in water source towards less permeable and slower subsurface flowpaths that sustain flow during the driest parts of the year. The predominance of young water routed along fast flowpaths suggests a rapid connection between these upstream headwaters to downstream perennial waters, indicating that changes to water quality and/or quantity in non-perennial streams have the potential to cause significant downstream consequences.

Acknowledgments

Data and code associated with this study are available in the GitHub repository: https://github.com/LoganJaySwenson/Isotopes_Data-Code

References

Alexander, L. C. (2015). Science at the boundaries: scientific support for the Clean Water Rule. *Freshwater Science*, *34*(4), 1588–1594. https://doi.org/10.1086/684076

Allen, D. C., Datry, T., Boersma, K. S., Bogan, M. T., Boulton, A. J., Bruno, D., et al. (2020). River ecosystem conceptual models and non-perennial rivers: A critical review. *WIREs Water*, *7*(5), e1473. https://doi.org/10.1002/wat2.1473

504   Botter, G., & Durighetto, N. (2020). The Stream Length Duration Curve: A Tool for Characterizing

505   the Time Variability of the Flowing Stream Length. *Water Resources Research*, *56*(8),

506   e2020WR027282. https://doi.org/10.1029/2020WR027282

507   Bowen, G. J. (2022). isoWater: Discovery, retrieval, and analysis of water isotope data (Version

508   1.1.1). Retrieved from https://CRAN.R-project.org/package=isoWater

509   Bowen, G. J., Putman, A., Brooks, J. R., Bowling, D. R., Oerter, E. J., & Good, S. P. (2018). Inferring

510   the source of evaporated waters using stable H and O isotopes. *Oecologia*, *187*(4), 1025–1039.

511   https://doi.org/10.1007/s00442-018-4192-5

512   Brookfield, A. e., Macpherson, G. l., & Covington, M. d. (2017). Effects of Changing Meteoric

513   Precipitation Patterns on Groundwater Temperature in Karst Environments. *Groundwater*,

514   *55*(2), 227–236. https://doi.org/10.1111/gwat.12456

515   Busch, M. H., Costigan, K. H., Fritz, K. M., Datry, T., Krabbenhoft, C. A., Hammond, J. C., et al. (2020).

516   What's in a Name? Patterns, Trends, and Suggestions for Defining Non-Perennial Rivers and

517   Streams. *Water*, *12*(7), 1980. https://doi.org/10.3390/w12071980

518   Byrnes, D. K., Van Meter, K. J., & Basu, N. B. (2020). Long-Term Shifts in U.S. Nitrogen Sources and

519   Sinks Revealed by the New TREND-Nitrogen Data Set (1930–2017). *Global Biogeochemical*

520   *Cycles*, *34*(9), e2020GB006626. https://doi.org/10.1029/2020GB006626

521   Cornwall, W. (2020, April 23). 'Hydrologists should be happy.' Big Supreme Court ruling bolsters

522   groundwater science. *Science*. Retrieved from

523   https://www.science.org/content/article/scotus-clean-water

524   Costigan, K. H., Daniels, M. D., & Dodds, W. K. (2015). Fundamental spatial and temporal

525   disconnections in the hydrology of an intermittent prairie headwater network. *Journal of*

526   *Hydrology*, *522*, 305–316. https://doi.org/10.1016/j.jhydrol.2014.12.031

527   Costigan, K. H., Jaeger, K. L., Goss, C. W., Fritz, K. M., & Goebel, P. C. (2016). Understanding controls

528   on flow permanence in intermittent rivers to aid ecological research: integrating meteorology,

529   geology and land cover. *Ecohydrology*, *9*(7), 1141–1153. https://doi.org/10.1002/eco.1712

530   Craig, H. (1961). Isotopic Variations in Meteoric Waters. *Science*, *133*(3465), 1702–1703.

531   https://doi.org/10.1126/science.133.3465.1702

532   Dansgaard, W. (1964). Stable isotopes in precipitation. *Tellus*, *16*(4), 436–468.

533   https://doi.org/10.1111/j.2153-3490.1964.tb00181.x

534   Datry, T., Truchy, A., Olden, J. D., Busch, M. H., Stubbington, R., Dodds, W. K., et al. (2023). Causes,

535   Responses, and Implications of Anthropogenic versus Natural Flow Intermittence in River

536   Networks. *BioScience*, *73*(1), 9–22. https://doi.org/10.1093/biosci/biac098

537   von Freyberg, J., Allen, S. T., Seeger, S., Weiler, M., & Kirchner, J. W. (2018). Sensitivity of young

538   water fractions to hydro-climatic forcing and landscape properties across 22 Swiss catchments.

539   *Hydrology and Earth System Sciences*, *22*(7), 3841–3861. https://doi.org/10.5194/hess-22-

540   3841-2018

541   Glenn, C. R., Whittier, R. B., Dailer, M. L., Dulaiova, H., El-Kadi, A. I., Fackrell, J., et al. (2013). Lahaina

542   groundwater tracer study -- Lahaina, Maui, Hawaii. Retrieved from

543   http://hdl.handle.net/10125/50768

544   Gómez, R., Arce, M. I., Baldwin, D. S., & Dahm, C. N. (2017). Chapter 3.1 - Water Physicochemistry

545   in Intermittent Rivers and Ephemeral Streams. In T. Datry, N. Bonada, & A. Boulton (Eds.),

546   *Intermittent Rivers and Ephemeral Streams* (pp. 109–134). Academic Press.

547   https://doi.org/10.1016/B978-0-12-803835-2.00005-X

548   Hale, R. L., & Godsey, S. E. (2019). Dynamic stream network intermittence explains emergent

549   dissolved organic carbon chemostasis in headwaters. *Hydrological Processes*, *33*(13), 1926–

550   1936. https://doi.org/10.1002/hyp.13455

551   Hammond, J. C., Zimmer, M., Shanafield, M., Kaiser, K., Godsey, S. E., Mims, M. C., et al. (2021).

552   Spatial Patterns and Drivers of Nonperennial Flow Regimes in the Contiguous United States.

553   *Geophysical Research Letters*, *48*(2), e2020GL090794. https://doi.org/10.1029/2020GL090794

554   Hatley, C. M., Armijo, B., Andrews, K., Anhold, C., Nippert, J. B., & Kirk, M. F. (2023). Intermittent

555   streamflow generation in a merokarst headwater catchment. *Environmental Science:

556   Advances*, *2*(1), 115–131. https://doi.org/10.1039/D2VA00191H

557   Hayden, B. P. (n.d.). Regional climate and the distribution of tallgrass prairie. In A. K. Knapp, J. M.

558   Briggs, D. C. Hartnett, & S. L. Collins (Eds.), *Grassland Dynamics* (pp. 19–34). New York: Oxford

559   University Press.

560   Hrachowitz, M., Benettin, P., van Breukelen, B. M., Fovet, O., Howden, N. J. K., Ruiz, L., et al. (2016).

561   Transit times—the link between hydrology and water quality at the catchment scale. *WIREs

562   Water*, *3*(5), 629–657. https://doi.org/10.1002/wat2.1155

563   Jasechko, S. (2019). Global Isotope Hydrogeology—Review. *Reviews of Geophysics*, *57*(3), 835–965.

564   https://doi.org/10.1029/2018RG000627

565   Jasechko, S., Kirchner, J. W., Welker, J. M., & McDonnell, J. J. (2016). Substantial proportion of

566   global streamflow less than three months old. *Nature Geoscience*, *9*(2), 126–129.

567   https://doi.org/10.1038/ngeo2636

568   Jensen, C. K., McGuire, K. J., McLaughlin, D. L., & Scott, D. T. (2019). Quantifying spatiotemporal

569   variation in headwater stream length using flow intermittency sensors. *Environmental*

570   *Monitoring and Assessment*, *191*(4), 226. https://doi.org/10.1007/s10661-019-7373-8

571   Keen, R. M., Nippert, J. B., Sullivan, P. L., Ratajczak, Z., Ritchey, B., O'Keefe, K., & Dodds, W. K.

572   (2022). Impacts of Riparian and Non-riparian Woody Encroachment on Tallgrass Prairie

573   Ecohydrology. *Ecosystems*. https://doi.org/10.1007/s10021-022-00756-7

574   Kirchner, J. W. (2016a). Aggregation in environmental systems – Part 1: Seasonal tracer

575   cycles quantify young water fractions, but not mean transit times, in spatially heterogeneous

576   catchments. *Hydrology and Earth System Sciences*, *20*(1), 279–297.

577   https://doi.org/10.5194/hess-20-279-2016

578   Kirchner, J. W. (2016b). Aggregation in environmental systems – Part 2: Catchment mean

579   transit times and young water fractions under hydrologic nonstationarity. *Hydrology and Earth*

580   *System Sciences*, *20*(1), 299–328. https://doi.org/10.5194/hess-20-299-2016

581   Koundouri, P., Boulton, A. J., Datry, T., & Souliotis, I. (2017). Chapter 5.2 - Ecosystem Services,

582   Values, and Societal Perceptions of Intermittent Rivers and Ephemeral Streams. In T. Datry, N.

583   Bonada, & A. Boulton (Eds.), *Intermittent Rivers and Ephemeral Streams* (pp. 455–476).

584   Academic Press. https://doi.org/10.1016/B978-0-12-803835-2.00018-8

585   Krabbenhoft, C. A., Allen, G. H., Lin, P., Godsey, S. E., Allen, D. C., Burrows, R. M., et al. (2022).

586   Assessing placement bias of the global river gauge network. *Nature Sustainability*, *5*(7), 586–

587   592. https://doi.org/10.1038/s41893-022-00873-0

588   Lutz, S. R., Krieg, R., Müller, C., Zink, M., Knöller, K., Samaniego, L., & Merz, R. (2018). Spatial

589   Patterns of Water Age: Using Young Water Fractions to Improve the Characterization of

590   Transit Times in Contrasting Catchments. *Water Resources Research*, *54*(7), 4767–4784.

591   https://doi.org/10.1029/2017WR022216

592   Macpherson, G. L. (1996). Hydrogeology of thin limestones: the Konza Prairie Long-Term Ecological

593   Research Site, Northeastern Kansas. *Journal of Hydrology*, *186*(1), 191–228.

594   https://doi.org/10.1016/S0022-1694(96)03029-6

595   Macpherson, G. L., & Sullivan, P. L. (2019). Watershed-scale chemical weathering in a merokarst
596   terrain, northeastern Kansas, USA. *Chemical Geology*, *527*, 118988.
597   https://doi.org/10.1016/j.chemgeo.2018.12.001
598   Macpherson, G. L., Roberts, J. A., Blair, J. M., Townsend, M. A., Fowle, D. A., & Beisner, K. R. (2008).
599   Increasing shallow groundwater CO2 and limestone weathering, Konza Prairie, USA.
600   *Geochimica et Cosmochimica Acta*, *72*(23), 5581–5599.
601   https://doi.org/10.1016/j.gca.2008.09.004
602   McDonnell, J. J., Spence, C., Karran, D. J., van Meerveld, H. J. (Ilja), & Harman, C. J. (2021). Fill-and-
603   Spill: A Process Description of Runoff Generation at the Scale of the Beholder. *Water*
604   *Resources Research*, *57*(5), e2020WR027514. https://doi.org/10.1029/2020WR027514
605   McGuire, K. J., & McDonnell, J. J. (2006). A review and evaluation of catchment transit time
606   modeling. *Journal of Hydrology*, *330*(3), 543–563.
607   https://doi.org/10.1016/j.jhydrol.2006.04.020
608   Messager, M. L., Lehner, B., Cockburn, C., Lamouroux, N., Pella, H., Snelder, T., et al. (2021). Global
609   prevalence of non-perennial rivers and streams. *Nature*, *594*(7863), 391–397.
610   https://doi.org/10.1038/s41586-021-03565-5
611   Meter, K. J. V., Basu, N. B., Veenstra, J. J., & Burras, C. L. (2016). The nitrogen legacy: emerging
612   evidence of nitrogen accumulation in anthropogenic landscapes. *Environmental Research*
613   *Letters*, *11*(3), 035014. https://doi.org/10.1088/1748-9326/11/3/035014
614   National Ecological Observatory Network (NEON). (2022a). Stable isotopes in precipitation
615   (DP1.00038.001). National Ecological Observatory Network (NEON).
616   https://doi.org/10.48443/E3MY-7V57
617   National Ecological Observatory Network (NEON). (2022b). Stable isotopes in surface water
618   (DP1.20206.001). National Ecological Observatory Network (NEON).
619   https://doi.org/10.48443/YZ7H-F560
620   Nippert, J. (2022). AWEOL Meteorlogical data from the Konza prairie headquarters weather station.
621   Environmental Data Initiative. Retrieved from
622   http://dx.doi.org/10.6073/pasta/98b9d0a612c17ab9f8f121d9741e72a6
623   Ransom, M. D., Rice, C. W., & Todd, T. C. (n.d.). Soils and soil biota. In A. K. Knapp, J. M. Briggs, D. C.
624   Hartnett, & S. L. Collins (Eds.), *Grassland Dynamics: Long-term ecological research in tallgrass*
625   *praire* (pp. 48–66). New York: Oxford University Press.

Rusjan, S., Sapač, K., Petrič, M., Lojen, S., & Bezak, N. (2019). Identifying the hydrological behavior of a complex karst system using stable isotopes. *Journal of Hydrology*, *577*, 123956. https://doi.org/10.1016/j.jhydrol.2019.123956

Segura, C. (2021). Snow drought reduces water transit times in headwater streams. *Hydrological Processes*, *35*(12), e14437. https://doi.org/10.1002/hyp.14437

Segura, C., Noone, D., Warren, D., Jones, J. A., Tenny, J., & Ganio, L. M. (2019). Climate, Landforms, and Geology Affect Baseflow Sources in a Mountain Catchment. *Water Resources Research*, *55*(7), 5238–5254. https://doi.org/10.1029/2018WR023551

Shanafield, M., Bourke, S. A., Zimmer, M. A., & Costigan, K. H. (2021). An overview of the hydrology of non-perennial rivers and streams. *WIREs Water*, *8*(2), e1504. https://doi.org/10.1002/wat2.1504

Staudinger, M., Seibert, J., & van Meerveld, H. J. (2021). Representation of Bi-Directional Fluxes Between Groundwater and Surface Water in a Bucket-Type Hydrological Model. *Water Resources Research*, *57*(9), e2020WR028835. https://doi.org/10.1029/2020WR028835

Stubbington, R., Acreman, M., Acuña, V., Boon, P. J., Boulton, A. J., England, J., et al. (2020). Ecosystem services of temporary streams differ between wet and dry phases in regions with contrasting climates and economies. *People and Nature*, *2*(3), 660–677. https://doi.org/10.1002/pan3.10113

Sullivan, P. L., Stops, M. W., Macpherson, G. L., Li, L., Hirmas, D. R., & Dodds, W. K. (2019). How landscape heterogeneity governs stream water concentration-discharge behavior in carbonate terrains (Konza Prairie, USA). *Chemical Geology*, *527*, 118989. https://doi.org/10.1016/j.chemgeo.2018.12.002

Sullivan, Pamela L., Zhang, C., Behm, M., Zhang, F., & Macpherson, G. L. (2020). Toward a new conceptual model for groundwater flow in merokarst systems: Insights from multiple geophysical approaches. *Hydrological Processes*, *34*(24), 4697–4711. https://doi.org/10.1002/hyp.13898

Tramblay, Y., Rutkowska, A., Sauquet, E., Sefton, C., Laaha, G., Osuch, M., et al. (2021). Trends in flow intermittence for European rivers. *Hydrological Sciences Journal*, *66*(1), 37–49. https://doi.org/10.1080/02626667.2020.1849708

Tsypin, M., & Macpherson, G. L. (2012). The effect of precipitation events on inorganic carbon in soil and shallow groundwater, Konza Prairie LTER Site, NE Kansas, USA. *Applied Geochemistry*, *27*(12), 2356–2369. https://doi.org/10.1016/j.apgeochem.2012.07.008

658   Van Meter, K. J., Van Cappellen, P., & Basu, N. B. (2018). Legacy nitrogen may prevent achievement

659   of water quality goals in the Gulf of Mexico. *Science*, *360*(6387), 427–430.

660   https://doi.org/10.1126/science.aar4462

661   Vero, S. e., Macpherson, G. l., Sullivan, P. l., Brookfield, A. e., Nippert, J. b., Kirk, M. f., et al. (2018).

662   Developing a Conceptual Framework of Landscape and Hydrology on Tallgrass Prairie:A Critical

663   Zone Approach. *Vadose Zone Journal*, *17*(1), 170069. https://doi.org/10.2136/vzj2017.03.0069

664   Vu, H. M., Shanafield, M., & Batelaan, O. (2018). Flux dynamics at the groundwater-surface water

665   interface in a tropical catchment. *Limnologica*, *68*, 36–45.

666   https://doi.org/10.1016/j.limno.2017.06.003

667   Wade, J., Kelleher, C., Ward, A. S., & Schewe, R. L. (2022). The fluid definition of the 'waters of the

668   United States': Non-uniform effects of regulation on US wetland protections. *Hydrological

669   Processes*, *36*(11), e14747. https://doi.org/10.1002/hyp.14747

670   Walsh, R., & Ward, A. S. (2022). An overview of the evolving jurisdictional scope of the U.S. Clean

671   Water Act for hydrologists. *WIREs Water*, *9*(5), e1603. https://doi.org/10.1002/wat2.1603

672   Ward, A. S., Zarnetske, J. P., Baranov, V., Blaen, P. J., Brekenfeld, N., Chu, R., et al. (2019). Co-

673   located contemporaneous mapping of morphological, hydrological, chemical, and biological

674   conditions in a 5th-order mountain stream network, Oregon, USA. *Earth System Science Data*,

675   *11*(4), 1567–1581. https://doi.org/10.5194/essd-11-1567-2019

676   Ward, A. S., Wade, J., Kelleher, C., & Schewe, R. L. (2023). Clarify jurisdiction of US Clean Water Act.

677   *Science*, *379*(6628), 148–148. https://doi.org/10.1126/science.adf7391

678   Warix, S. R., Godsey, S. E., Lohse, K. A., & Hale, R. L. (2021). Influence of groundwater and

679   topography on stream drying in semi-arid headwater streams. *Hydrological Processes*, *35*(5),

680   e14185. https://doi.org/10.1002/hyp.14185

681   Zimmer, M. A., & McGlynn, B. L. (2017). Bidirectional stream–groundwater flow in response to

682   ephemeral and intermittent streamflow and groundwater seasonality. *Hydrological Processes*,

683   *31*(22), 3871–3880. https://doi.org/10.1002/hyp.11301

684   Zimmer, M. A., & McGlynn, B. L. (2018). Lateral, Vertical, and Longitudinal Source Area Connectivity

685   Drive Runoff and Carbon Export Across Watershed Scales. *Water Resources Research*, *54*(3),

686   1576–1598. https://doi.org/10.1002/2017WR021718

687   Zipper, S., Popescu, I., Compare, K., Zhang, C., & Seybold, E. C. (2022). Alternative stable states and

688   hydrological regime shifts in a large intermittent river. *Environmental Research Letters*, *17*(7),

689   074005. https://doi.org/10.1088/1748-9326/ac7539

690   Zipper, S. C., Hammond, J. C., Shanafield, M., Zimmer, M., Datry, T., Jones, C. N., et al. (2021).

691   Pervasive changes in stream intermittency across the United States. *Environmental Research*

692   *Letters*, *16*(8), 084033. https://doi.org/10.1088/1748-9326/ac14ec

Supplementary Information

SI1. Detailed Methods:
SI1.1 Sampling strategy

The 50 sampling sites in this study were defined to leverage existing long-term data while spanning a range of watershed physiographic and no-flow conditions. In addition to the water isotope samples investigated in this study, these sampling sites were also used for a variety of other samples including microbial and macroinvertebrate communities, other water chemistry parameters, and instrumentation with stream temperature, intermittency, and conductivity (STIC) sensors, and therefore the sampling approach used was meant to balance the competing priorities of these teams, rather than optimize the sampling from a purely isotope-driven perspective.

First, we identified a subset of priority locations that we wanted to ensure were sampled. These priority locations included sites with existing hydrological data including long-term weirs maintained by the Konza LTER network (n=4), existing stream intermittency sensors from other projects (n=10, which included our planned watershed outlet location), locations immediately downstream of a subset of springs identified during field mapping campaigns (n=7), and near unmonitored tributary junctions (n=2). Combined, these priority locations made up 23 of our sampling sites.

For the remaining 27 sites, we distributed sampling sites using a stratified random sampling approach spanning two variables that have previously been shown to influence stream intermittency: topographic wetness index (TWI) and drainage area (Warix et al., 2021). TWI is a unitless physiographic variable that integrates drainage area and local slope, and locations with higher TWI values are locations that may be wetter due to the accumulation of water from upslope areas. To distribute the points randomly, we first discretized the stream network into equally spaced points at 2 m resolution, which matches the resolution of the DEM used to create the stream network map. We then binned these points into 10 bins that had approximately equal width at the lower end of the drainage area distribution, where points were more densely concentrated, and approximately the same number of total stream points at the higher end of the drainage area distribution, where points were less densely concentrated (Figure S1).

To obtain 50 total sampling points spanning a range of TWI and drainage area conditions, we attempted to place 5 sampling sites within each drainage area bin that spanned the range of TWI values within that bin. To accomplish this, for each drainage area bin we split the range of TWI into 5 quantiles, which we refer to here as bin-quantiles. We identified how many priority locations were already within each bin-quantile and randomly selected a point on the stream network within each bin-quantile, ensuring that it was $\geq$ 100 m from any existing sampling site. If the priority sites included multiple sampling sites within a given bin-quantile, we could not place a sampling site in each of the bin-quantiles, in which case we randomly selected bin-quantiles to reach a total of 5 sampling sites within that drainage area bin. There were 6 bin-quantiles that we were unable to select sampling sites because all points within that bin-quantil were within 100 m of an existing sampling site. These remaining 6 sampling sites were placed by manually inspecting the stream network and identifying substantial gaps. We then made slight adjustments to some of the sampling sites that were randomly located, for example moving the location from downstream to upstream of a road crossing and/or further back from a tributary junction.

The final distribution of the 50 sampling sites with respect to drainage area and TWI is shown in Figure S2 and Figure S3. Figure 1 shows the spatial distribution of the sampling sites within the stream network.
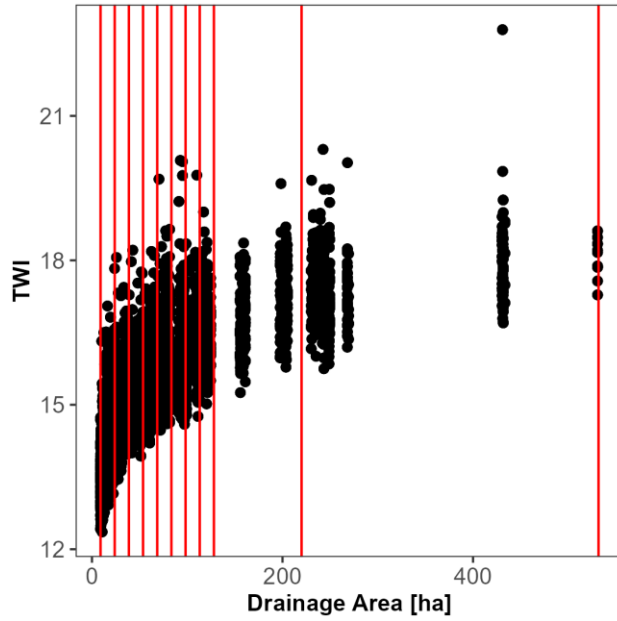
Figure S1. Distribution of drainage area and TWI for all stream network points at the site. The red vertical lines indicate the 10 drainage area groups used to randomly distribute points, and each bin was divided into 5 quantiles based on the TWI distribution.
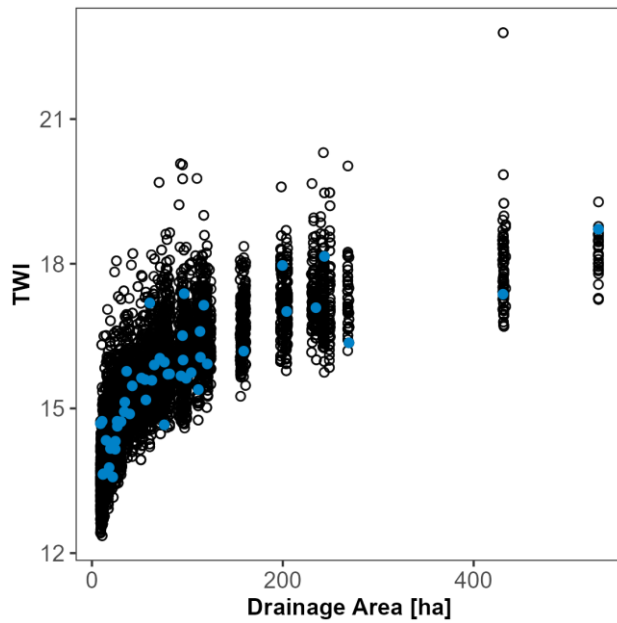
Figure S2. Distribution of drainage area and TWI for sampling sites (blue) and all stream network points (black) at the site.
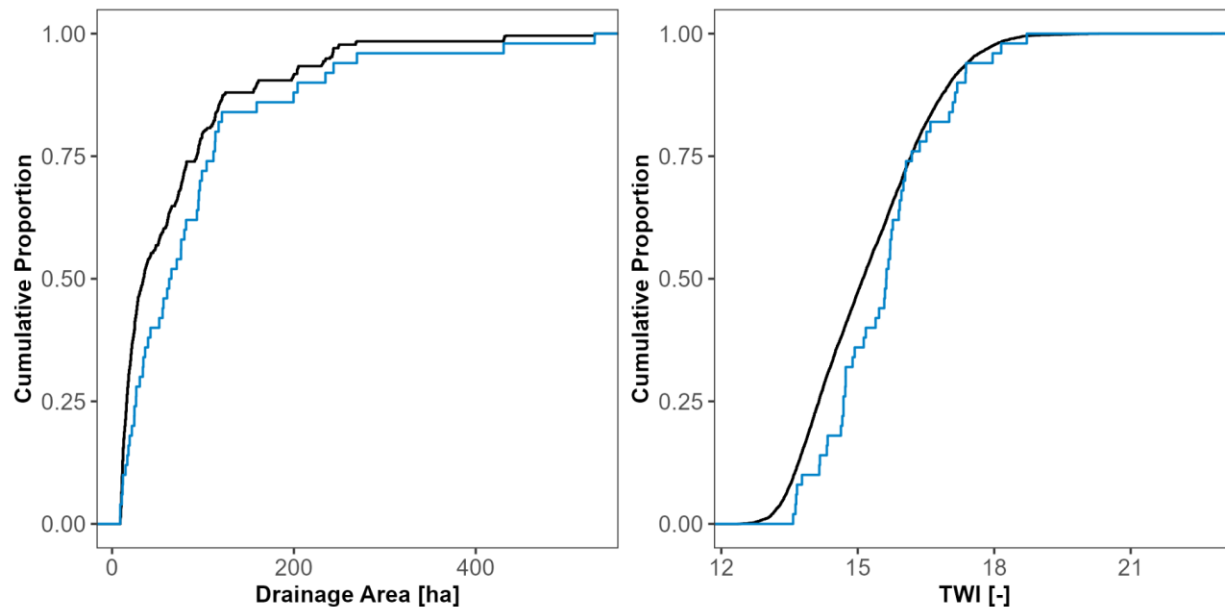
Figure S3. Empirical cumulative distribution functions (ECDFs) of drainage area and TWI for all stream points (black) and sampling sites (blue) for the site.

SI1.2 Random forest to predict δ^{18}O compositions

We developed a random forest model to predict stream δ^{18}O ratios and to quantify the factors that most strongly influence δ^{18}O during the summer dry-down of the South Fork of Kings Creek (i.e., the synoptic samples only) using the *party* package in R (Hothorn et al., 2006; Strobl et al., 2007; Strobl et al., 2008). Random forest models are particularly well-suited for hydrological prediction due to their ability to handle numerous predictors with potentially nonlinear and interacting relationships, relatively low risk of overfitting, and ease in interpreting the importance of each input variable (Eng et al., 2017; Addor et al., 2018; Miller et al., 2018). We developed a random forest model to predict δ^{18}O across all sites and sampling dates using the following predictor variables: day of year (i.e., date of sampling event), flow state (i.e., whether flowing or pooled), water temperature, topographic wetness index, contributing area, burn frequency, elevation, and slope. We then extracted the conditional permutation importance for each predictor variable (Strobl et al., 2008), which accounts for collinearity among other predictors. A higher conditional variable importance indicates that the predictor variable has a greater influence on model predictors for the out-of-bag samples used in model training. Lastly, we calculated the root mean squared error (RMSE) between the predicted δ^{18}O and the observed δ^{18}O to assess model performance. We found that day of year, flow state, and water temperature were the most influential predictor variables (Figure S6). This further supports our findings that evaporation and a decrease in surface water connectivity are the primary factors influencing stream δ^{18}O compositions (see Figure 5 in the main text).

SI2. Additional Results:
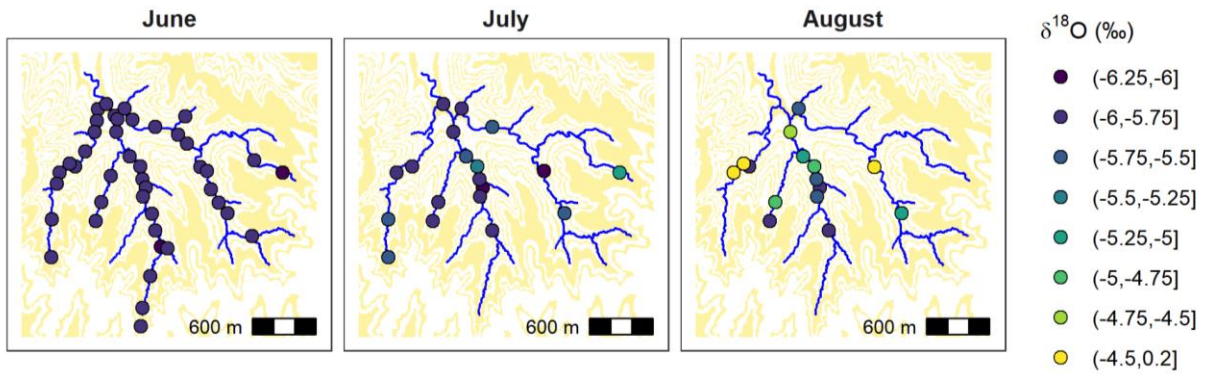
Figure S4. Spatial variation in $\delta^{18}O$ during the summer dry-down period. The estimated elevations at which limestone units outcrop the watershed are shown as yellow bands. These elevations are based on the average member thickness in the drilling log records at the Konza Prairie.
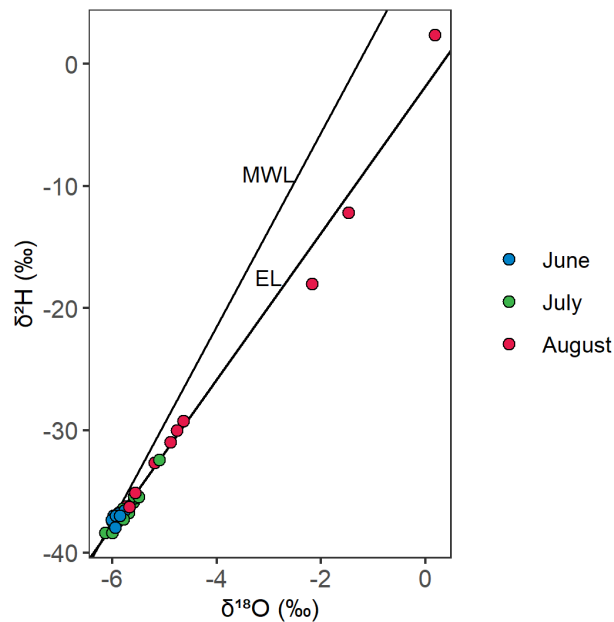
Figure S5. Stream $\delta^{18}O$ and δ^2H in the South Fork of Kings Creek. Shown are the meteoric water line (MWL) and the evaporation line (EL).
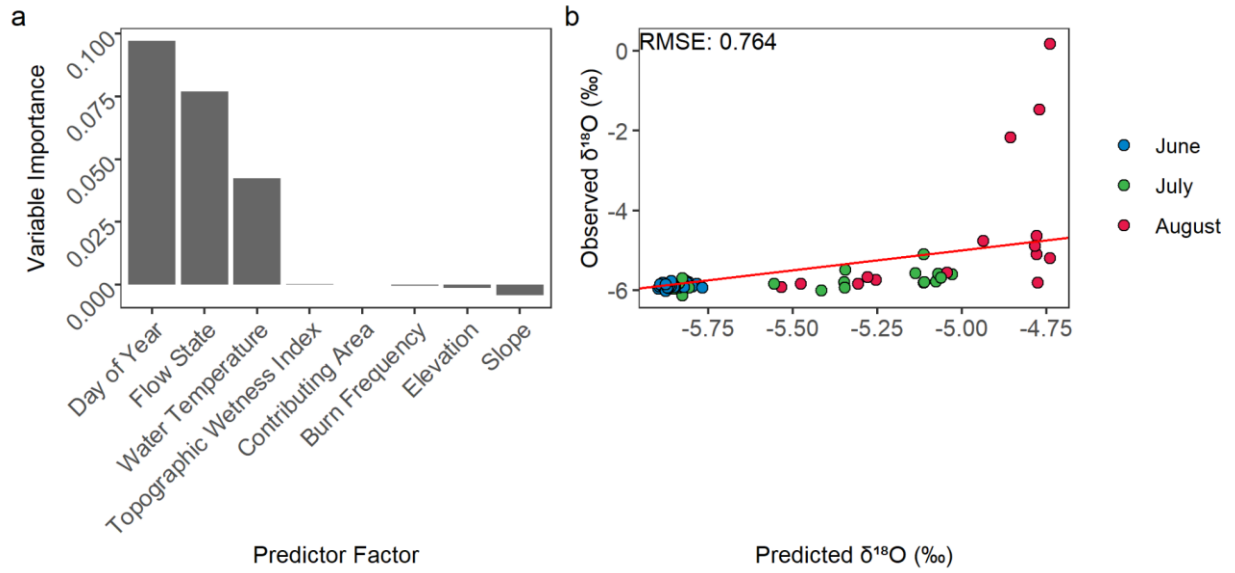
Figure S6. Random forest model to predict $\delta^{18}O$ in the South Fork of Kings Creek. Shown are (a) predictor factors ordered according to decreasing conditional permutation importance and (b) model fit.
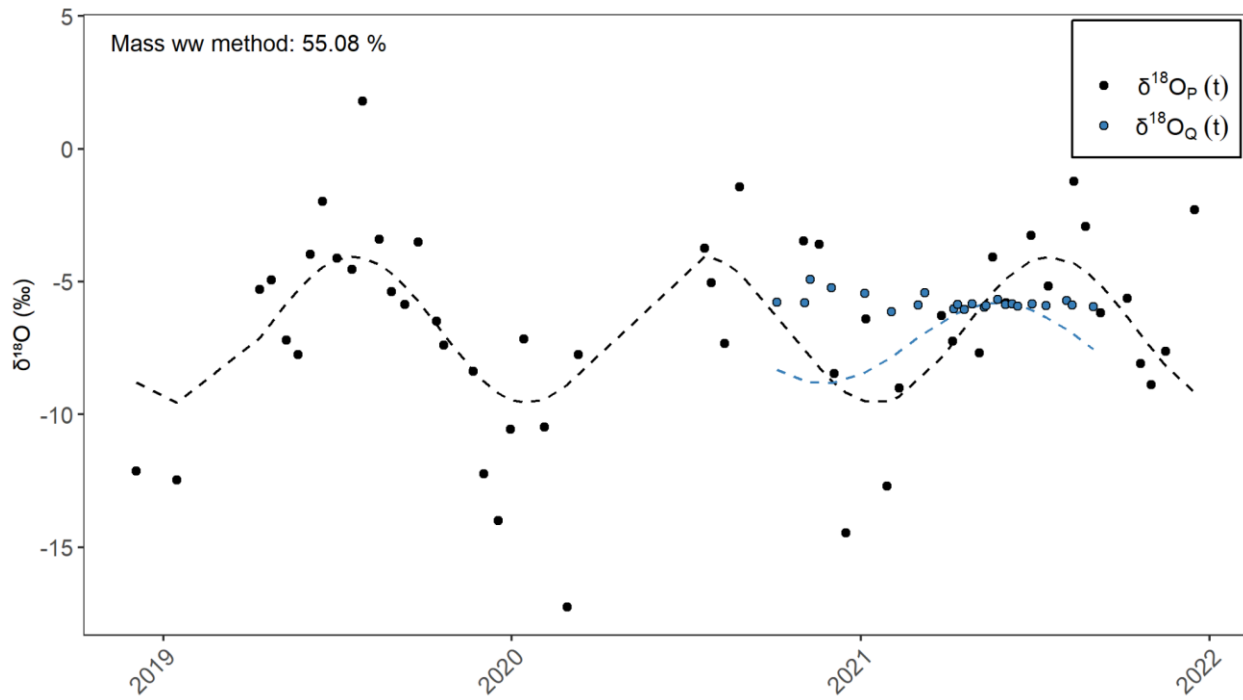
Figure S7. Sinusoidal amount-weighted model fits for $\delta^{18}O_P(t)$ and $\delta^{18}O_Q(t)$ (Eq. 1 and 2).
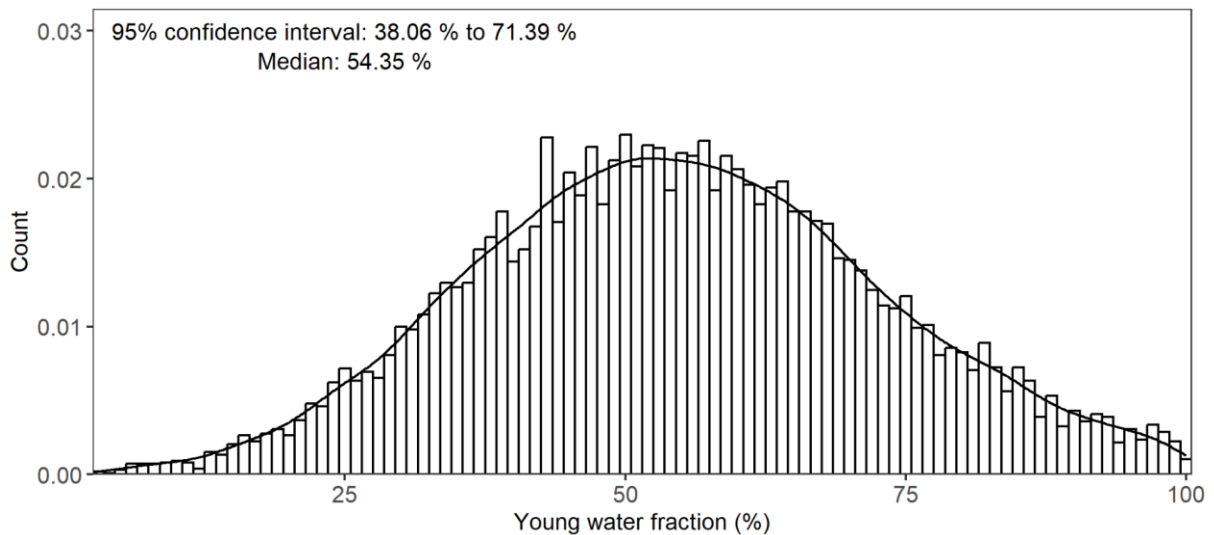
Figure S8. Uncertainty in the F_{YW} assessed 10,000 times (Eq. 3) by generating random errors in the original precipitation and streamwater isotope data and fitting the disturbed data to sinusoidal models for $\delta^{18}O_P(t)$ and $\delta^{18}O_Q(t)$ (Eq. 1 and 2), respectively (similar to Lutz et al., 2016). The original data were disturbed using a normal distribution of the random errors with a standard deviation equal to 5% of the range of observed $\delta^{18}O$ values.

Supplementary References

Addor, N., Nearing, G., Prieto, C., Newman, A. J., Le Vine, N., & Clark, M. P. (2018). A Ranking of Hydrological Signatures Based on Their Predictability in Space. *Water Resources Research*, *54*(11), 8792–8812. https://doi.org/10.1029/2018WR022606

Eng, K., Grantham, T. E., Carlisle, D. M., & Wolock, D. M. (2017). Predictability and selection of hydrologic metrics in riverine ecohydrology. *Freshwater Science*, *36*(4), 915–926. https://doi.org/10.1086/694912

Hothorn, T., Bühlmann, P., Dudoit, S., Molinaro, A., & Van Der Laan, M. J. (2006). Survival ensembles. *Biostatistics*, *7*(3), 355–373. https://doi.org/10.1093/biostatistics/kxj011

Lutz, S. R., Krieg, R., Müller, C., Zink, M., Knöller, K., Samaniego, L., & Merz, R. (2018). Spatial Patterns of Water Age: Using Young Water Fractions to Improve the Characterization of Transit Times in Contrasting Catchments. *Water Resources Research*, *54*(7), 4767–4784. https://doi.org/10.1029/2017WR022216

Miller, M. P., Carlisle, D. M., Wolock, D. M., & Wieczorek, M. (2018). A Database of Natural Monthly Streamflow Estimates from 1950 to 2015 for the Conterminous United States. *JAWRA Journal of the American Water Resources Association*, *54*(6), 1258–1269. https://doi.org/10.1111/1752-1688.12685

Strobl, C., Boulesteix, A.-L., Zeileis, A., & Hothorn, T. (2007). Bias in random forest variable importance measures: Illustrations, sources and a solution. *BMC Bioinformatics*, *8*(1), 25. https://doi.org/10.1186/1471-2105-8-25

Strobl, C., Boulesteix, A.-L., Kneib, T., Augustin, T., & Zeileis, A. (2008). Conditional variable importance for random forests. *BMC Bioinformatics*, *9*(1), 307. https://doi.org/10.1186/1471-2105-9-307

Warix, S. R., Godsey, S. E., Lohse, K. A., & Hale, R. L. (2021). Influence of groundwater and topography on stream drying in semi-arid headwater streams. *Hydrological Processes*, *35*(5), e14185. https://doi.org/10.1002/hyp.14185